Eur. Phys. J. C 49, 665–674 (2007)
DOI 10.1140/epjc/s10052-006-0152-z

THE EUROPEAN PHYSICAL JOURNAL C

Regular Article – Theoretical Physics

Form factors and branching ratio for the $B \to l\nu\gamma$ decay

M.S. Khan, M.J. Aslam, A.H.S. Gilani, Riazuddin[a]

National Center for Physics, Quaid-i-Azam University, Islamabad 45320, Pakistan

Received: 20 June 2006 /
Published online: 8 December 2006 – © Springer-Verlag / Società Italiana di Fisica 2006

Abstract. Form factors parameterizing radiative leptonic decays of heavy mesons $\left(B^+ \to \gamma l^+ \nu_l\right)$ against photon energy are computed in the language of dispersion relations. The states contributing to the absorptive part in the dispersion relation are the multiparticle continuum, estimated by the quark triangle graph, and resonances with quantum numbers 1^- and 1^+, which includes B^* and B_A^* and their radial excitations, which model the higher state contributions. Constraints provided by the asymptotic behavior of the structure dependent amplitude, Ward identities and gauge invariance are used to provide useful information for the parameters needed. The couplings $g_{BB^*\gamma}$ and $f_{BB_A^*\gamma}$ are predicted as we restrict ourselves to the first radial excitation; otherwise using these as an input the radiative decay coupling constants for the radial excitations are predicted. The value of the branching ratio for the process $B^+ \to \gamma\mu^+\nu_\mu$ is found to be in the range 0.5×10^{-6}. A detailed comparison is given with other approaches.

1 Introduction

In spite of the small branching ratio, the radiative B-meson decay $(B \to l\nu\gamma)$ is of viable interest, because it contains important information about the weak and hadronic interactions of the B-meson. Furthermore, with the introduction of the B-factories LHCb, BaBar, Belle and CLEOb, the radiative B-meson decay can be studied with enough statistics. Preliminary data from the CLEO Collaboration indicate that the limit on the branching ratio $\mathcal{B}(B \to l\nu\gamma)$ is

$$\mathcal{B}(B \to e\nu_e\gamma) < 2.0 \times 10^{-4}\,,$$
$$\mathcal{B}(B \to \mu\nu_\mu\gamma) < 5.2 \times 10^{-5}\,,$$

at 90% confidence level [1, 2]. With the better statistics expected from the upcoming B-factories, the observation and experimental study of this decay could soon become feasible. It is therefore of some interest to have good theoretical control over the theoretical uncertainties affecting the relevant matrix elements.

The radiative leptonic decay $B^+ \to l^+\nu_l\gamma$ has received a great deal of attention in the literature [3–14] as a means of probing the aspects of the strong and weak interactions of a heavy quark system. The presence of the additional photon in the final state can compensate for the helicity suppression of the decay rate present in the purely leptonic mode. As a result, the branching ratio for the radiative leptonic mode can be as large as 10^{-6} for the μ^+ case [11], which would open up the possibility for directly measuring the decay constant f_B [8]. A study of this decay can offer also useful information about the Cabibbo–Kobayashi–Maskawa (CKM) matrix element $|V_{ub}|$ [15, 16].

In the radiative B-decay process, there are two contributions to the amplitude:

1. inner bremsstrahlung (IB) and
2. the structure dependent (SD) contribution which depends on the vector and axial vector form factor F_V and F_A respectively.

The IB contribution to the decay amplitude is associated with the tree diagrams shown in Fig. 1a and b, and the SD contribution is associated with Fig. 1c.

In this paper, we will study the radiative leptonic B-decays of $B^+ \to l^+\nu_l\gamma$. The IB part is still helicity suppressed [3], while the SD one is free from the suppression [17]. Therefore, the radiative decay rates of $B^+ \to l^+\nu_l\gamma$ $(l = e, \mu)$ could have an enhancement with respect to the purely leptonic modes of $B^+ \to l^+\nu_l$ due to the SD contributions in spite of the electromagnetic coupling constant α. With the possible large branching ratios, the radiative leptonic B-decays could be measured in future experiments at the hadronic colliders, such as BTeV and the CERN large hadron collider (LHC-B) experiments [18].

The paper is organized as follows. In Sect. 2, we present the decay kinematics and current matrix elements for $B^+ \to l^+\nu_l\gamma$. In Sect. 3, we discuss the various contributions to the absorptive part of the SD amplitude $\mathrm{i}H_{\mu\nu}$, needed in the dispersion relation. This includes the multiparticle continuum and resonances with the quantum numbers 1^- and 1^+. The resonances include B^*- and B_A^*-mesons and their radial excitations, which model the higher states. The continuum is estimated by quark trian-

[a] e-mail: riazuddin@ncp.edu.pk

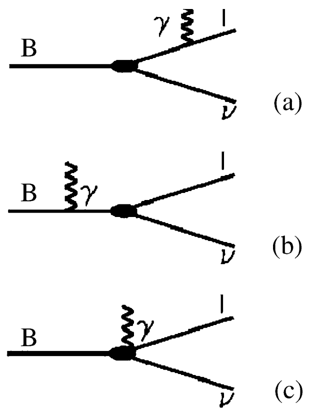

Fig. 1. $B \to l\nu_l\gamma$ radiative leptonic decay diagrams

gle graphs. In Sect. 4, the asymptotic behavior of the SD amplitude is studied. This provides a usual constraint on the residues of the resonance contribution, in terms of the continuum contribution. In Sect. 5, we discuss the Ward identities which together with gauge invariance relate various form factors. These identities, which are expected to hold below the resonance regime, fix the normalization of the form factors at $q^2 = 0$ in terms of the universal function $g_+(0)$ as well as another constraint on the residues. Thus, in our approach, a parametrization of the q^2 dependence of the form factors is not approximated by a single pole contribution. But this parametrization is dictated by considerations mentioned above and also predicts the coupling constants of 1^- and 1^+ resonances with the photon if we restrict ourselves to one radial excitation; otherwise, using these as input, the radiative coupling constants of the radial excitations are predicted. In this and other respects our approach is different from the others mentioned previously. Our approach is closest to the one used in [19] for $B \to \pi l \nu_l$. We calculate the decay branching ratios in Sect. 6. We give our conclusions in Sect. 7.

2 Decay kinematics and current matrix elements

We consider the decay

$$B^+(p) \to l^+(p_l)\nu_l(p_\nu)\gamma(k)\,, \tag{1}$$

where l stands for e or μ, and γ is a real photon with $k^2 = 0$. The decay amplitude for the radiative leptonic decay $B^+ \to l^+\nu_l\gamma$ can be written in two parts, M_{IB} and M_{SD}, as follows:

$$M(B^+ \to l^+\nu_l\gamma) = M_{\mathrm{IB}} + M_{\mathrm{SD}}\,, \tag{2}$$

in terms of two emission types of the real photon from $B^+ \to l^+\nu_l$. They are given by [20–23]

$$M_{\mathrm{IB}} = \mathrm{i}e\frac{G_{\mathrm{F}}}{\sqrt{2}}V_{ub}f_B m_l \epsilon^*_\mu L^\mu\,, \tag{3}$$

$$M_{\mathrm{SD}} = -\mathrm{i}\frac{G_{\mathrm{F}}}{\sqrt{2}}V_{ub}f_B m_l \epsilon^*_\mu \tilde{H}^{\mu\nu} l_\nu\,, \tag{4}$$

with

$$L^\mu = m_l \bar{u}(p_\nu)\,(1+\gamma_5)\left(\frac{2p^\mu}{2pk} - \frac{2p_l^\mu + \not{k}\gamma^\mu}{2p_l k}\right) v(p_l, s_l)\,, \tag{5}$$

$$l^\mu = \bar{u}(p_\nu)\gamma^\mu\,(1+\gamma_5)\,v(p_l, s_l)\,, \tag{6}$$

$$\tilde{H}^{\mu\nu} = \mathrm{i}F_{\mathrm{V}}(q^2)\epsilon^{\mu\nu\alpha\beta}k_\alpha p_\beta - F_{\mathrm{A}}(q^2)\,(pkg^{\mu\nu} - p^\mu k^\nu)\,, \tag{7}$$

$$q^\mu = (p-k)^\mu = (p_l + p_\nu)^\mu\,. \tag{8}$$

Here ϵ^*_μ denotes the polarization vector of the photon with $k^\mu \epsilon^*_\mu(k) = 0$. p, p_l, p_ν, and k are the four-momenta of B^+, l^+, ν, and γ, respectively; s_l is the polarization vector of the l^+, f_B is the B-meson decay constant, and F_{A}, F_{V} stand for two Lorentz invariant amplitudes (form factors).

The term proportional to L^μ in (5) does not contain unknown quantities – it is determined by the amplitude of the non-radiative decay $B^+ \to l^+\nu_l$. This part of the amplitude is usually referred as the “inner bremsstrahlung contribution”, whereas the term proportional to $H^{\mu\nu}$ is called a “structure dependent contribution”.

The form factor F_{A} (F_{V}) is related to the matrix element of the axial (vector) current. The factors f_B and $F_{\mathrm{V,A}}$ are defined by

$$\langle 0\,|\bar{u}\gamma^\mu\gamma_5 b|\,B(p)\rangle = -\mathrm{i}f_B p^\mu\,, \tag{9}$$

$$\langle \gamma\,(k)\,|\bar{u}\gamma^\mu\gamma_5 b|\,B(p)\rangle = -\left[(\epsilon^* p)\,k^\mu - \epsilon^{*\mu}\,(pk)\right]F_{\mathrm{A}}(q^2)\,, \tag{10}$$

$$\langle \gamma\,(k)\,|\bar{u}\gamma^\mu b|\,B(p)\rangle = -\mathrm{i}\epsilon^{\mu\nu\alpha\beta}\epsilon^*_\nu p_\alpha k_\beta F_{\mathrm{V}}(q^2)\,. \tag{11}$$

In our phase convention, the form factors F_{A} and F_{V} are real in the physical region,

$$m_l^2 \ll q^2 \ll M_B^2\,,$$

where q is the momentum transfer. The kinematics of the decay needs two variables, for which we choose the conventional quantities, and in the rest frame of B,

$$x = \frac{2pk}{M_B^2} = \frac{2E_\gamma}{M_B}\,, \tag{12}$$

$$y = \frac{2pp_l}{M_B^2} = \frac{2E_l}{M_B}\,, \tag{13}$$

and the angle $\theta_{l\gamma}$ between the photon and the charged lepton is related to x and y by

$$x = \frac{1}{2}\frac{\left(2-y+\sqrt{y^2-4r_l}\right)\left(2-y-\sqrt{y^2-4r_l}\right)}{2-y+\sqrt{y^2-4r_l}\cos\theta_{l\gamma}}\,. \tag{14}$$

In terms of these quantities, one can write the momentum transfer as

$$q^2 = M_B^2(1-x) \quad (k^2 = 0)\,. \tag{15}$$

We write the physical region of x and y as

$$0 \le x \le 1 - r_l\,, \tag{16}$$

$$1 - x + \frac{r_l}{1-x} \le y \le 1 + r_l\,, \tag{17}$$

where

$$r_l = \frac{m_l^2}{M_B^2} = \begin{cases} 9.329 \times 10^{-9} & (l=e)\,, \\ 4.005 \times 10^{-4} & (l=\mu)\,. \end{cases} \tag{18}$$

3 Dispersion relations

The structure dependent part, $H^{\mu\nu}$ is given by

$$\mathrm{i}H^{\mu\nu} = \mathrm{i}\int \mathrm{d}^4 x e^{\mathrm{i}kx} \left\langle 0 \left| T\left(j^\mu_{\mathrm{em}}(x) J_2^\nu(0)\right)\right| B(p)\right\rangle \,. \tag{19}$$

We note that [24]

$$\mathrm{i}k_\mu H^{\mu\nu} = \mathrm{i} f_B p_\nu\,, \tag{20}$$

so that for the real photon we can write

$$H^{\mu\nu} = \tilde{H}^{\mu\nu} + f_B \frac{p^\mu p^\nu}{pk}\,, \tag{21}$$

where $k_\mu \tilde{H}^{\mu\nu} = 0$ and $\tilde{H}^{\mu\nu}$ is parametrized as in (7). The second term in (21) is absorbed in M_{IB}. The absorptive part is

$$\begin{aligned} &\mathrm{Abs}\left[\mathrm{i}H^{\mu\nu}\right] \\ &= \frac{1}{2}\int \mathrm{d}^4 x \mathrm{e}^{\mathrm{i}kx} \left\langle 0 \left| \left[j^\mu_{\mathrm{em}}(x), J_2^\nu(0)\right]\right| B(p)\right\rangle \\ &= \frac{1}{2}(2\pi)^4 \Big[\sum_n \left\langle 0 \left| j^\mu_{\mathrm{em}}(0)\right| n\right\rangle \left\langle n \left| J_2^\nu(0)\right| B(p)\right\rangle \delta^4(k-p_n) \\ &\quad - \sum_n \left\langle 0 \left| J_2^\nu(0)\right| n\right\rangle \left\langle n \left| j^\mu_{\mathrm{em}}(0)\right| B(p)\right\rangle \delta^4(k+p_n-p)\Big] \,. \end{aligned} \tag{22}$$

The δ-function in the first term implies that only values with $p_n^2 = k^2 = 0$ are relevant, and since there is no real particle with zero mass, the first term does not contribute. Thus contributing to the absorptive part are all possible intermediate states that couple to $B\gamma$ and annihilated by the weak vertex $\langle 0 | J_2^\nu(0) | n\rangle$. These include the multiparticle continuum as well as resonances with quantum numbers 1^- and 1^+. Thus $(t = q^2)$

$$\begin{aligned} F_{\mathrm{V}}(t) &= \frac{g_{BB^*\gamma}}{M^2_{B^*} - t} f_{B^*} + \ldots \\ F_{\mathrm{A}}(t) &= \frac{f_{B^*_A B\gamma}}{M^2_{B^*_A} - t} f_{B^*_A} + \ldots\,. \end{aligned} \tag{23}$$

The ellipses stand for contributions from higher states with the same quantum numbers. The couplings $g_{BB^*\gamma}$ and $f_{B^*_A B\gamma}$ are defined as

$$\begin{aligned} \left\langle B^{*-}(q,\eta)\gamma\,(k,\epsilon)\mid B^-(P)\right\rangle &= \mathrm{i}g_{B^*B\gamma}\varepsilon_{\alpha\rho\mu\sigma}\epsilon^{*\alpha}q^\rho\eta^{*\mu}p^\sigma\,, \\ \left\langle B^{*-}_A(q,\eta)\gamma\,(k,\epsilon)\mid B^-(P)\right\rangle &= \mathrm{i}g_{B^*_A B\gamma}(\epsilon^*\eta^*) \\ &\quad - \mathrm{i}f_{B^*_A B\gamma}(q\epsilon^*)(k\eta^*)\,, \\ \left\langle 0 \left| \mathrm{i}\bar{u}\gamma^\mu b \right| B^*(q,\eta)\right\rangle &= f_{B^*}\eta^\mu\,, \\ \left\langle 0 \left| \mathrm{i}\bar{u}\gamma^\mu\gamma_5 b \right| B^*_A(q,\eta)\right\rangle &= f_{B^*_A}\eta^\mu\,. \end{aligned} \tag{24}$$

We assume that the contributions from the radial excitations of B^* and B^*_A dominate the higher state contribution. Thus we write

$$\begin{aligned} F_{\mathrm{V}}(t) &= \frac{R_V}{1 - t/M^2_{B^*}} + \sum_i \frac{R_{V_i}}{1-t/M^2_{B^*_i}} \\ &\quad + \frac{1}{\pi}\int_{S_0}^{M^2} \frac{\mathrm{Im}\, F_{\mathrm{V}}^{\mathrm{Cont}}(s)}{s - t - \mathrm{i}\varepsilon}\mathrm{d}s + \ldots\,, \\ F_{\mathrm{A}}(t) &= \frac{R_A}{1 - t/M^2_{B^*_A}} + \sum_i \frac{R_{A_i}}{1-t/M^2_{B^*_{A_i}}} \\ &\quad + \frac{1}{\pi}\int_{S_0}^{M^2} \frac{\mathrm{Im}\, F_{\mathrm{A}}^{\mathrm{Cont}}(s)}{s - t - \mathrm{i}\varepsilon}\mathrm{d}s + \ldots\,, \end{aligned} \tag{25}$$

where the ellipses stand for the contributions from the region for with much larger mass than the physical mass of the heavy resonances up to ∞. Here, M is a cut off near the first radial excitation of M_{B^*} or $M_{B^*_A}$ and $S_0 = M_B + m_\pi$, and

$$\begin{aligned} R_V &= \frac{g_{BB^*\gamma}}{M^2_{B^*}} f_{B^*}\,, \\ R_A &= \frac{f_{B^*_A B\gamma}}{M^2_{B^*_A}} f_{B^*_A}\,. \end{aligned} \tag{26}$$

R_{V_i} and R_{A_i} are the corresponding quantities for the radial excitations with masses $M_{B^*_i}$ and $M_{B^*_{A_i}}$. In the next section we develop the constraints on some of the parameters appearing in the above equations.

If we model the continuum contribution by a quark triangular graph (similar calculations exist in the literature [25, 26]), we obtain

$$\begin{aligned} F_{\mathrm{V}}^{\mathrm{Cont}} = F_{\mathrm{A}}^{\mathrm{Cont}} &= \frac{f_B}{M_B}\left\{\frac{Q_u}{\bar{\Lambda}} - \frac{Q_b}{M_B}\left(1 + \frac{\bar{\Lambda}}{M_B}\right)\right\} \\ &\quad \times \frac{1}{1 - q^2/M_B^2}\,, \end{aligned} \tag{27}$$

where

$$\bar{\Lambda} = M_B - m_b\,, \tag{28}$$

together with the term

$$(Q_u - Q_b) f_B \frac{p^\mu p^\nu}{kp} = f_B \frac{p^\mu p^\nu}{kp}\,,$$

which appears in (21). As is well known (see for example [27, 28]), the pole at $q^2 = M_B^2$ in (27) arises due to the u $(\bar{b})$ quark propagator which forms one leg of the quark Δ; the other legs are part of the B-meson wave function.

4 Asymptotic behavior

To get constraints on the residues R_i, it is useful to study the asymptotic behavior of the form factors F_{V} and F_{A}. It has been argued that the behavior of the form factor for very large values of $|t|$ can be estimated reliably in perturbative QCD processes [pQCD] [19, 29–32]. For $t \ll 0$, and for $|t|$ much larger than the physical mass of the heavy resonances, pQCD should yield a very good approximation to the form factors. First we note that by vector meson dominance

$$\begin{aligned}&\langle \gamma(k, \varepsilon^*(k))| \bar{u}\gamma^\mu (1-\gamma_5) b | B(p)\rangle \\ &\simeq Q_u \frac{f_\rho}{m_\rho} \langle \rho(k, \varepsilon^*(k))| \bar{u}\gamma^\mu (1-\gamma_5) b | B(p)\rangle\,, \end{aligned} \tag{29}$$

where f_ρ, having the dimension of mass, is defined as

$$\langle 0 | \bar{u}\gamma^\mu u | \rho(k, \varepsilon(k))\rangle = \frac{f_\rho}{m_\rho}\varepsilon^\mu\,. \tag{30}$$

Then using the methods employed in [31, 32], it is easy to calculate [only the diagram where a gluon is emitted by the light quark in the $(b\bar{u})$ bound state and absorbed by the heavy quark contributes and is by itself gauge invariant] F^{pQCD}:

$$\begin{aligned}F_{\mathrm{V}}^{\mathrm{pQCD}} &= F_{\mathrm{A}}^{\mathrm{pQCD}} \\ &= \left(Q_u \frac{f_\rho}{m_\rho}\right)\frac{32\pi\alpha_{\mathrm{s}}(t)}{3}(f_B f_\rho)\, m_B \left(\frac{1}{\varepsilon}\ln\varepsilon\right)\frac{1}{t^2}\,.\end{aligned} \tag{31}$$

Here

$$\varepsilon \sim \mathcal{O}\left(\frac{\Lambda_{\mathrm{QCD}}}{m_B}\right), \tag{32}$$

It is governed by the tail end of the B-meson wave function characterized by ε.

Now the asymptotic behavior of (25) is given by

$$\begin{aligned}&F(q^2) \to \\ &-\frac{1}{q^2}\left[RM^2 + \sum_i R_i M_i^2 + \frac{1}{\pi}\int_{S_0}^{M^2} \operatorname{Im} F^{\mathrm{Cont}}(s)\,\mathrm{d}s\right].\end{aligned} \tag{33}$$

Since $F^{\mathrm{pQCD}}(t)$ is a reliable approximation to the form factor for $t \to -\infty$, and $\left(tF^{\mathrm{pQCD}}\right) \to 0$ in this limit, it follows that

$$RM^2 + \sum_i R_i M_i^2 + c \simeq 0\,, \tag{34}$$

where we have defined

$$c = \frac{1}{\pi}\int_{S_0}^{M^2} \operatorname{Im} F^{\mathrm{Cont}}(s)\,\mathrm{d}s\,. \tag{35}$$

The convergence relation (34) is a model independent result and constitutes a very binding constraint for model building. In other words, the various contributions in (33) may be individually much larger than the $\left(tF^{\mathrm{pQCD}}(t)\right)$ due to $\alpha_{\mathrm{s}}(t)/t$ suppression, but there must be large cancellations among the non-perturbative contributions in (33). This is in the spirit of [19]. We will explore the resonant contribution (in our model) in order to understand the effect of (34) on the behavior of form factors in the physical region. The imposition of this constraint will lead to a very distinct behavior of the photon momentum distribution, independently of how many resonances we choose to keep. As the radial excitations of B^* become heavier, they are less relevant to the form factors since the spacing between the consecutive radial excitations are expected to become narrower and narrower [33]. Thus, heavier resonances contribute with a smaller value even in the narrow width approximation. Furthermore, as finite widths are considered, the contribution of heavier and thus broader excitations are additionally suppressed. This shows that the truncation of the sum over resonances is a reasonable approximation.

For the reasons stated above we will study a constrained dispersive model where only the first two radial excitations are kept. This is mainly for the reason mentioned above. On the other hand, the “minimal” choice of keeping only one radial excitation will determine R_1 in terms of R. The other necessary ingredient to specify the model is knowledge of the spectrum of radial excitations. These resonances [$(2S)$ and $(3S)$ excitations of B^*] have not yet been observed in the B systems. We will then rely on potential model calculations for their masses [33]. These models have been very successful in predicting the masses of orbitally excited states, and therefore we are confident that the position of the radial excitations does not introduce a sizeable uncertainty. The resultant spectrum explicitly shows that the spacing among the $1S$, $2S$, $3S$ states are, to leading order, independent of the heavy quark mass and, therefore, constitute the property of the light degrees of freedom. The spectrum of radial excitations is given in Table 1, where the subindices 1 and 2 correspond to the $2S$ and $3S$ excitation of the B^*, etc. Thus the convergence condition (34) now reads

$$RM^2 + R_1 M_1^2 + R_2 M_2^2 + c = 0\,. \tag{36}$$

This condition leaves two free parameters R_1 and R_2 in the model. This results in the correct scaling of form factors with the heavy meson mass. Solving (36) for R_2 and using this in (33), we obtain

$$\begin{aligned}F(q^2) &= \frac{RM^2\left(M_2^2 - M^2\right)}{\left(M^2 - q^2\right)\left(M_2^2 - q^2\right)} + \frac{R_1 M_1^2\left(M_2^2 - M_1^2\right)}{\left(M_1^2 - q^2\right)\left(M_2^2 - q^2\right)} \\ &\quad + \frac{1}{M_2^2 - q^2}\frac{1}{\pi}\int_{S_0}^{M^2} \frac{M_2^2 - s}{s - q^2}\operatorname{Im} F_{\mathrm{V}}^{\mathrm{Cont}}\,.\end{aligned} \tag{37}$$

Table 1. B-meson masses in GeV [35, 36]

	J^P	M	M_1/M	M_2/M
M_B	0^-	5.28	1.14	1.24
M_{B^*}	1^-	5.33	1.14	1.24
$M_{B_A^*}$	1^+	5.71	1.12	1.22

If we model the continuum contribution by a quark triangle graph as given in (27), we obtain

$$F\left(q^2\right)=\frac{RM^2\left(M_2^2-M^2\right)}{\left(M^2-q^2\right)\left(M_2^2-q^2\right)}+\frac{R_1M_1^2\left(M_2^2-M_1^2\right)}{\left(M_1^2-q^2\right)\left(M_2^2-q^2\right)} +\frac{M_2^2-M^2}{\left(M_2^2-q^2\right)\left(M^2-q^2\right)}c\,, \tag{38}$$

where in the heavy quark limit $M_B=M_B^*=M$ and

$$c=f_BM_B\left[\frac{Q_u}{\bar{\Lambda}}+\mathcal{O}\left(\frac{1}{M_B}\right)\right]. \tag{39}$$

5 Ward identity constraints

It is useful to define

$$\langle\gamma\left(k,\epsilon\right)|\bar{u}\mathrm{i}\sigma^{\mu\nu}q_\nu b|\,B(p)\rangle=-\mathrm{i}\varepsilon^{\mu\nu\alpha\beta}\epsilon_\nu^*k_\alpha p_\beta F_1(q^2)\,, \tag{40}$$

$$\langle\gamma\left(k,\epsilon\right)|\bar{u}\mathrm{i}\sigma^{\mu\nu}\gamma_5q_\nu b|\,B(p)\rangle=\left[\left(qk\right)\epsilon^{*\mu}-\left(\epsilon^*q\right)k^\mu\right]F_3(q^2)\,. \tag{41}$$

Now we will make use of the Ward identities and gauge invariance principle to relate different form factors.

Usually, gauge invariance is implemented by means of the Ward identities; another way, essentially the same, is to consider what happens if the polarization vector of an external (real) photon is replaced by its four-momentum. The result is zero, provided that one considers all diagrams where this particular photon is connected in all possible ways to a charge carrying line. In this way one understands the connection between gauge invariance and charge conservation. The Ward identities[1] used to relate different form factors appearing in our process are

$$\begin{aligned}&\langle\gamma\left(k,\epsilon\right)|\bar{u}\mathrm{i}\sigma^{\mu\nu}q_\nu b|\,B(p)\rangle\\&=-(m_b+m_q)\left\langle\gamma\left(k,\epsilon\right)|\bar{u}\gamma^\mu b|\,B(p)\right\rangle\\&\quad+(p^\mu+k^\mu)\left\langle\gamma\left(k,\epsilon\right)|\bar{u}b|\,B(p)\right\rangle\\&=-(m_b+m_q)\left\langle\gamma\left(k,\epsilon\right)|\bar{u}\gamma^\mu b|\,B(p)\right\rangle\,,\end{aligned} \tag{42}$$

$$\begin{aligned}&\langle\gamma\left(k,\epsilon\right)|\bar{u}\mathrm{i}\sigma^{\mu\nu}\gamma_5q_\nu b|\,B(p)\rangle\\&=(m_b-m_q)\left\langle\gamma\left(k,\epsilon\right)|\bar{u}\gamma^\mu\gamma_5 b|\,B(p)\right\rangle\\&\quad+(p^\mu+k^\mu)\left\langle\gamma\left(k,\epsilon\right)|\bar{u}\gamma_5b|\,B(p)\right\rangle\\&=(m_b-m_q)\left\langle\gamma\left(k,\epsilon\right)|\bar{u}\gamma^\mu\gamma_5 b|\,B(p)\right\rangle\,,\end{aligned} \tag{43}$$

where the matrix elements $\langle\gamma(k,\epsilon)\,|\bar{u}b|\,B(p)\rangle$ and $\langle\gamma(k,\epsilon)$ $|\bar{u}\gamma_5b|\,B(p)\rangle$ vanish for a real photon due to gauge invariance.

Using the Ward identities in (40) and (41), and comparing the coefficients, we obtain $[pk=qk,\ \epsilon^*p=\epsilon^*q]$

$$F_{\mathrm{V}}(q^2)=\frac{1}{m_b+m_q}F_1(q^2)\,, \tag{44}$$

$$F_{\mathrm{A}}(q^2)=\frac{1}{m_b-m_q}F_3(q^2)\,. \tag{45}$$

[1] See [34] for a detailed derivation of these Ward identities.

The results given in (44) and (45) are model independent, because these are derived by using the Ward identities.

In order to make use of the Ward identities to relate different form factors, we define

$$\begin{aligned}&\langle\gamma\left(k,\epsilon\right)|\mathrm{i}\bar{u}\sigma_{\alpha\beta}b|\,B(p)\rangle\\&=-\mathrm{i}\varepsilon_{\alpha\beta\rho\sigma}\epsilon^{*\rho}(k)\left[(p+k)^\sigma g_++q^\sigma g_-\right]\\&-\mathrm{i}q\epsilon^*(k)\varepsilon_{\alpha\beta\rho\sigma}(p+k)^\rho q^\sigma h\\&-\mathrm{i}\left[q_\alpha\varepsilon_{\beta\rho\sigma\tau}\epsilon^{*\rho}(k)(p+k)^\sigma q^\tau-\alpha\leftrightarrow\beta\right]h_1\\&-\mathrm{i}\left[(p+k)_\alpha\,\varepsilon_{\beta\rho\sigma\tau}\epsilon^{*\rho}(k)\,(p+k)^\sigma\,q^\tau-\alpha\leftrightarrow\beta\right]h_2\,.\end{aligned} \tag{46}$$

Since we have a real photon, gauge invariance requires that if we replace $\epsilon^\mu(k)$ by k^μ, the matrix element should vanish. This requires

$$g_++g_-+2\left(qk\right)h=0\,. \tag{47}$$

From the Dirac algebra

$$\sigma^{\mu\nu}\gamma_5=-\frac{\mathrm{i}}{2}\varepsilon^{\mu\nu\alpha\beta}\sigma_{\alpha\beta}\,, \tag{48}$$

we can write

$$\begin{aligned}&\langle\gamma\left(k,\epsilon\right)|\mathrm{i}\bar{u}\sigma^{\mu\nu}\gamma_5b|\,B(p)\rangle\\&=-\frac{\mathrm{i}}{2}\varepsilon^{\mu\nu\alpha\beta}\left\langle\gamma(k,\epsilon)\,|\mathrm{i}\bar{u}\sigma_{\alpha\beta}b|\,B(p)\right\rangle\\&=\left(\epsilon^{*\mu}k^\nu-\epsilon^{*\nu}k^\mu\right)\\&\quad\times\left[g_+-g_--\left(M_B^2+q^2\right)h_1-\left(3M_B^2-q^2\right)h_2\right]\\&\quad+\left(\epsilon^{*\mu}p^\nu-\epsilon^{*\nu}p^\mu\right)\left[g_++g_-+\left(M_B^2-q^2\right)(h_1+h_2)\right]\\&\quad-2q\epsilon^*\left(h-h_1-h_2\right)\left(p^\mu k^\nu-p^\nu k^\mu\right)\,.\end{aligned} \tag{49}$$

By gauge invariance, namely, replacing ϵ^μ by k^μ, the matrix element should be zero, and this does not give any new relation other than (47). Using this relation and $2kq=M_B^2-q^2$, we get

$$\begin{aligned}&\langle\gamma\left(k,\epsilon\right)|\mathrm{i}\bar{u}\sigma^{\mu\nu}\gamma_5b|\,B(p)\rangle=\left(\epsilon^{*\mu}k^\nu-\epsilon^{*\nu}k^\mu\right)\\&\times\left[2g_++\left(M_B^2-q^2\right)(h-h_1-h_2)-2q^2h_1-2M_B^2h_2\right]\\&-\left[2kq\left(\epsilon^{*\mu}p^\nu-\epsilon^{*\nu}p^\mu\right)+2q\epsilon^*\left(p^\mu k^\nu-p^\nu k^\mu\right)\right]\\&\times\left(h-h_1-h_2\right).\end{aligned} \tag{50}$$

Contrary to what is stated in the literature, the gauge invariance does allow a second tensor structure in addition to $(\epsilon^\mu k^\nu-\epsilon^\nu k^\mu)$.

This gives

$$\begin{aligned}&\langle\gamma\left(k,\epsilon\right)|\mathrm{i}\bar{q}\sigma^{\mu\nu}q_\nu\gamma_5b|\,B(p)\rangle\\&=2\left(g_+-q^2h-\left(M_B^2-q^2\right)h_2\right)\left(qk\epsilon^{*\mu}\left(k\right)-q\epsilon^*\left(k\right)k^\mu\right)\,.\end{aligned} \tag{51}$$

This, in turn, gives [from (41)]

$$F_3(q^2)=2\left[-g_+-q^2h-\left(M_B^2-q^2\right)h_2\right]\,. \tag{52}$$

Similarly, from (46), we get the relation

$$\begin{aligned}&\left\langle\gamma\left(k,\epsilon\right)\left|\bar{u}\mathrm{i}\sigma_{\alpha\beta}q^\beta b\right|B(p)\right\rangle\\&=-\mathrm{i}\varepsilon_{\alpha\beta\rho\sigma}\epsilon^{*\rho}q^\beta p^\sigma 2\left[g_+-q^2h_1-M_B^2h_2\right]\,.\end{aligned}$$

Comparison of this equation with (40) gives

$$F_1\left(q^2\right)=2[g_+\left(q^2\right)-q^2h_1\left(q^2\right)-M_B^2h_2\left(q^2\right)]\,. \quad (53)$$

Thus, finally we obtain

$$F_{\mathrm{V}}\left(q^2\right)=\frac{2}{m_b+m_q}\left\{g_+\left(q^2\right)-q^2h_1\left(q^2\right)-M_B^2h_2\left(q^2\right)\right\}\,, \quad (54)$$

$$F_{\mathrm{A}}\left(q^2\right)=\frac{2}{m_b-m_q} \times\left\{g_+\left(q^2\right)-q^2h\left(q^2\right)-\left(M_B^2-q^2\right)h_2\left(q^2\right)\right\}\,. \quad (55)$$

Therefore, the normalization of F_{V} and F_{A} at $q^2=0$ is determined by a universal form factor $\left(g_+(0)-M_B^2h_2\right)$. Now the form factor h_2 does not get any contribution from a quark triangle graph nor from the pole, and therefore we shall put it equal to zero. On the other hand, only $g_+\left(q^2\right)$ gets a contribution from the quark Δ graph – see [25, 26] for calculational details –

$$g_+\left(q^2\right)=f_B\left\{\frac{Q_u}{2\bar{\Lambda}}-\frac{Q_b}{2M_B}\left(1-\frac{m_q}{M_B}\right)\right\}\frac{1}{1-q^2/M_B^2}\,. \quad (56)$$

We expect the Ward identities to hold at low q^2 below the resonance regime and as such we use the results obtained from them at $q^2=0$. Thus from (54) and (55), we obtain

$$(m_b+m_q)\,F_{\mathrm{V}}(0)=2g_+(0)=(m_b-m_q)\,F_{\mathrm{A}}(0)\,. \quad (57)$$

Further, using (28) above, (57), and neglecting terms of the order of $\left(\bar{\Lambda}\mp m_q\right)/M_B$, we obtain another constraint using (38) and (39) at $q^2=0$:

$$R\left(1-\frac{M^2}{M_2^2}\right)+R_1\left(1-\frac{M_1^2}{M_2^2}\right)=\left(\frac{2g_+(0)}{M}\right)\frac{M^2}{M_2^2}\,. \quad (58)$$

Now if we restrict ourselves to one radial excitation $(M_2=M_1)$ we obtain from (58)

$$R=\frac{2g_+(0)}{\left(M_1^2/M^2-1\right)M} \quad (59)$$

$$F\left(q^2\right)=\frac{2}{M}\frac{g_+(0)}{\left(1-q^2/M^2\right)\left(1-q^2/M_1^2\right)}\,. \quad (60)$$

Restoring the subscripts and using the definitions (26)

$$g_{B^*B\gamma}=\frac{2g_+(0)}{M_B}\frac{M_{B^*}^2}{f_{B^*}\left(M_{B_1^*}^2/M_{B^*}^2-1\right)} \simeq\frac{2g_+(0)}{f_B\left(M_{B_1^*}^2/M_{B^*}^2-1\right)}\,, \quad (61)$$

while

$$f_{B_A^*B\gamma}=\frac{M_{B_A^*}^2}{M_B}\frac{2g_+(0)}{f_{B_A^*}\left(M_{B_{A_1}^*}^2/M_{B_A^*}^2-1\right)}\,. \quad (62)$$

Using $g_+(0)$ given in (56) with $Q_u=2/3$, namely

$$g_+(0)=\frac{2}{3}\frac{f_B}{2\bar{\Lambda}}\,, \quad (63)$$

we have the prediction

$$g_{B^*B\gamma}=\frac{2}{3\bar{\Lambda}}\frac{1}{\left(M_{B_1^*}^2/M_{B^*}^2-1\right)}\,. \quad (64)$$

Further

$$F_{\mathrm{V}}(q^2)=\frac{2}{M_B}\frac{g_+(0)}{\left(1-q^2/M_{B^*}^2\right)\left(1-q^2/M_{B_1^*}^2\right)}\,, \quad (65)$$

$$F_{\mathrm{A}}(q^2)=\frac{2}{M_B}\frac{g_+(0)}{\left(1-q^2/M_{B_A^*}^2\right)\left(1-q^2/M_{B_{A_1}^*}^2\right)}\,. \quad (66)$$

This is the final expression for the form factors of our process $B\to\gamma l\nu_l$, if we restrict ourselves to the one radial excitation. We also observe the approximate equality $F_{\mathrm{V}}(q^2)=F_{\mathrm{A}}(q^2)$ of the form factors which also occur in some other models [13, 14]. For numerical work, we shall use the B-meson masses given in Table 1 and $f_B=0.180$ GeV.

This gives the prediction from (64)

$$g_{B^*B\gamma}=\frac{2.2}{\bar{\Lambda}}=5.6\ \mathrm{GeV}^{-1}\,, \quad (67)$$

for $\bar{\Lambda}=5.28-4.8=0.4\ \mathrm{GeV}^{-1}$ [see (28) and Table 1]. Also, we obtain from (63)

$$g_+(0)=\frac{3}{20}=0.15\,. \quad (68)$$

Further from (62)

$$f_{B_A^*B\gamma}=\frac{f_BM_{B_A^*}}{f_{B_A^*}}\frac{2.6}{\bar{\Lambda}} =6.5\frac{f_BM_{B_A^*}}{f_{B_A^*}}\ \mathrm{GeV}^{-1}\,. \quad (69)$$

We now study the effect of the second radial excitation. We go back to (38) and use the constraint (58) to obtain

$$F\left(q^2\right) =\left[R\left(\frac{M_2^2}{M^2}-1\right)\left(\frac{M_1^2}{M^2}-1\right)\frac{M^2}{M_2^2}\frac{q^2}{M_1^2} +\frac{2g_+(0)}{M}\left(1-q^2\left(\frac{1}{M_2^2}+\frac{1}{M_1^2}-\frac{M^2}{M_1^2M_2^2}\right)\right)\right] /\left[\left(1-q^2/M_2^2\right)\left(1-q^2/M_1^2\right)\left(1-q^2/M^2\right)\right]\,.$$

If we parametrize R as

$$R=\frac{2g_+(0)}{M}\frac{1-\left(1-M_1^2/M_2^2\right)A}{\left(M_1^2/M^2-1\right)}\,,$$

where A is a parameter which in principle can be obtained when $g_{B^*B\gamma}$ and $f_{B_A^*B\gamma}$ become known. Then

$$F\left(q^2\right)=\frac{2g_+(0)}{M}\frac{1-\frac{q^2}{M_1^2}\left(1+\left(1-\frac{M^2}{M_2^2}\right)\left(1-\frac{M_1^2}{M_2^2}\right)A\right)}{\left(1-q^2/M_2^2\right)\left(1-q^2/M_1^2\right)\left(1-q^2/M^2\right)}. \tag{70}$$

For $M_1=M_2$ the above equation, (70), reduces to (60). So the couplings of B with $B^*\gamma$ and $B_A^*\gamma$ become

$$\begin{aligned} g_{B^*B\gamma}=&\frac{2g_+(0)M_{B^*}^2}{M_Bf_{B^*}\left(M_{B_1^*}^2/M_{B^*}^2-1\right)}\\ &\times\left[1-\left(1-M_{B^*}^2/M_{B_1^*}^2\right)\left(1-M_{B_1^*}^2/M_{B^*}^2\right)A\right]\\ =&\left[1-\left(1-M_{B^*}^2/M_{B_1^*}^2\right)\left(1-M_{B_1^*}^2/M_{B^*}^2\right)A\right]\\ &\times 5.6\ \mathrm{GeV}^{-1}, \end{aligned} \tag{71}$$

$$\begin{aligned} f_{B_A^*B\gamma}=&\frac{f_BM_{B_A^*}}{f_{B_A^*}}\\ &\times\left[1-\left(1-M_{B_A^*}^2/M_{B_{A_1}^*}^2\right)\left(1-M_{B_{A_1}^*}^2/M_{B_A^*}^2\right)A\right]\\ &\times 6.5\ \mathrm{GeV}^{-1}, \end{aligned} \tag{72}$$

and the corresponding form factors become

$$\begin{aligned} F_{\mathrm{V}}(q^2)=&\frac{2g_+(0)}{M_B}\\ &\times\frac{1-\frac{q^2}{M_{B_1^*}^2}\left(1+\left(1-\frac{M_{B^*}^2}{M_{B_2^*}^2}\right)\left(1-\frac{M_{B_1^*}^2}{M_{B_2^*}^2}\right)A\right)}{\left(1-q^2/M_{B_2^*}^2\right)\left(1-q^2/M_{B_1^*}^2\right)\left(1-q^2/M_{B^*}^2\right)}, \end{aligned} \tag{73}$$

$$\begin{aligned} F_{\mathrm{A}}(q^2)=&\frac{2g_+(0)}{M_B}\\ &\times\frac{1-\frac{q^2}{M_{B_{A_1}^*}^2}\left(1+\left(1-\frac{M_{B_A^*}^2}{M_{B_{A_2}^*}^2}\right)\left(1-\frac{M_{B_{A_1}^*}^2}{M_{B_{A_2}^*}^2}\right)A\right)}{\left(1-q^2/M_{B_{A_2}^*}^2\right)\left(1-q^2/M_{B_{A_1}^*}^2\right)\left(1-q^2/M_{B_A^*}^2\right)}. \end{aligned} \tag{74}$$

For the numerical values we shall use $A=0$ [i.e., $M_1=M_2$] and $A=3$ and $A=4.8$. The second value of $A(=3)$ corresponds to the estimate of $g_{B^*B\gamma}$ from vector meson dominance

$$g_{B^*B\gamma}=\frac{2}{3}g_{B^*B\rho^-}\frac{f_{\rho^-}}{m_\rho^2}=2.76\ \mathrm{GeV}^{-1},$$

where $g_{B^*B\rho^-}=\sqrt{2}(11)\ \mathrm{GeV}^{-1}$ obtained in [37,38] and $f_{\rho^-}/m_\rho=205\ \mathrm{MeV}$. The third value of $A(=4.8)$ gives more or less the width for $B^*\to B\gamma$ as obtained from the MI transition in the non-relativistic quark model (NRQM). These values give the decay width for the $B^*\to B\gamma$ transition as 23 keV, 5.5 keV and 0.8 keV, respectively, while the MI transition in NRQM predicts it to be 0.9 keV. These predictions are testable when the above decay width is experimentally measured.

6 Decay distribution

The Dalitz plot density

$$\begin{aligned} \rho(x,y)&=\frac{\mathrm{d}^2\Gamma}{\mathrm{d}x\,\mathrm{d}y}=\frac{\mathrm{d}^2\Gamma_{\mathrm{IB}}}{\mathrm{d}x\,\mathrm{d}y}+\frac{\mathrm{d}^2\Gamma_{\mathrm{SD}}}{\mathrm{d}x\,\mathrm{d}y}+\frac{\mathrm{d}^2\Gamma_{\mathrm{INT}}}{\mathrm{d}x\,\mathrm{d}y}\\ &=\rho_{\mathrm{IB}}(x,y)+\rho_{\mathrm{SD}}(x,y)+\rho_{\mathrm{INT}}(x,y) \end{aligned} \tag{75}$$

is a Lorentz invariant which contains the form factors F_{V} and F_{A} in the following form [20,21,23]:

$$\begin{aligned} &\rho_{\mathrm{IB}}(x,y)=A_{\mathrm{IB}}f_{\mathrm{IB}}(x,y),\\ &\rho_{\mathrm{SD}}(x,y)=A_{\mathrm{SD}}M_B^2\\ &\quad\times\left[(F_{\mathrm{V}}+F_{\mathrm{A}})^2f_{\mathrm{SD}^+}(x,y)+(F_{\mathrm{V}}-F_{\mathrm{A}})^2f_{\mathrm{SD}^-}(x,y)\right],\\ &\rho_{\mathrm{INT}}(x,y)=A_{\mathrm{INT}}M_B\\ &\quad\times\left[(F_{\mathrm{V}}+F_{\mathrm{A}})f_{\mathrm{INT}^+}(x,y)+(F_{\mathrm{V}}-F_{\mathrm{A}})f_{\mathrm{INT}^-}(x,y)\right], \end{aligned}$$

where

$$\begin{aligned} f_{\mathrm{IB}}(x,y)=&\left(\frac{1-y+r_l}{x^2(x+y-1-r_l)}\right)\\ &\times\left(x^2+2(1-x)(1-r_l)-\frac{2xr_l(1-r_l)}{(x+y-1-r_l)}\right),\\ f_{\mathrm{SD}^+}(x,y)=&(x+y-1-r_l)\left((x+y-1)(1-x)-r_l\right),\\ f_{\mathrm{SD}^-}(x,y)=&(1-y+r_l)\left((1-x)(1-y)+r_l\right),\\ f_{\mathrm{INT}^+}(x,y)=&\left(\frac{1-y+r_l}{x(x+y-1-r_l)}\right)\left((1-x)(1-x-y)+r_l\right),\\ f_{\mathrm{INT}^-}(x,y)=&\left(\frac{1-y+r_l}{x(x+y-1-r_l)}\right)\\ &\times\left(x^2-(1-x)(1-x-y)-r_l\right), \end{aligned}$$

and

$$\begin{aligned} A_{\mathrm{IB}}&=4r_l\left(\frac{f_B}{M_B}\right)^2A_{\mathrm{SD}},\\ A_{\mathrm{SD}}&=\frac{G_{\mathrm{F}}^2}{2}\frac{|V_{ub}|^2\alpha}{32\pi^2}M_B^5,\\ A_{\mathrm{INT}}&=4r_l\left(\frac{f_B}{M_B}\right)A_{\mathrm{SD}}. \end{aligned}$$

The SD^+ term reaches its maximum at $x=2/3$, $y=1$, which corresponds to $\theta_{l\gamma}=\pi$. The SD^- term reaches its maximum at $x=2/3$, $y=1/3$, corresponding to $\theta_{l\gamma}=0$. Indeed, for a lepton of maximal energy ($y=1$), only "right-handed" photons contribute. In this situation, the photon and the neutrino must be emitted in the direction opposite to that of the lepton. Angular momentum conservation forces the photon spin to be opposite to the total lepton spin, and the photon helicity has the same sign as that of the lepton. Then the photon and the neutrino are emitted parallel. This configuration corresponds to a neutrino of maximal energy ($E_\nu=E_\nu^{\max}$ when $x+y=1$). In this case, only the "left-handed" photon contributes. When $x+y=1$, the IB contribution becomes very large: this corresponds to $\theta_{l\gamma}=0$. Consequently, it is very difficult to distinguish experimentally between the IB and the SD^-

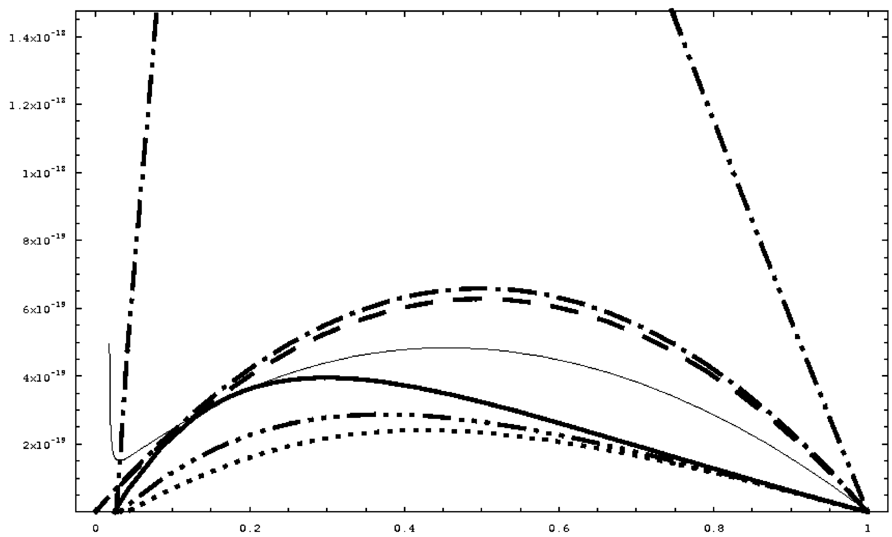

Fig. 2. The differential decay rate versus photon energy x is plotted and a comparison is given with various approaches. The *solid line* (for $A = 0$), the *dashed-triple-dotted line* (for $A = 3.0$) and the *dotted line* (for $A = 4.8$) are our calculation, the *dash-dot-dot line* is for [11], the *dashed line* for [13] and the *dash-dotted line* for [14]. The *thin-solid line* is the Sudakov resummation calculation result from [13]

contribution. To summarize, an experiment performed in the region $\theta_{l\gamma} \simeq \pi$ is essentially sensitive to $(F_\mathrm{V} + F_\mathrm{A})^2$.

The form factors calculated in (60) can be expressed in terms of the dimensionless variable x,

$$F(x) = \frac{F(0)}{x\left[1 - (1-x)/(M_1/M)^2\right]}, \tag{76}$$

where x is defined in (12) and q^2 in (15). After restoring subscripts, the form factors $F_\mathrm{V}\left(q^2\right)$ in (65) and $F_\mathrm{A}\left(q^2\right)$ in (66) can be written as

$$F_\mathrm{V}(x) = \frac{F_\mathrm{V}(0)}{x\left[1 - (1-x)/\left(M_{B_1^*}/M_{B^*}\right)^2\right]}, \tag{77}$$

$$F_\mathrm{A}(x) = \frac{F_\mathrm{V}(0)}{x\left[1 - (1-x)/\left(M_{B_{A_1}^*}/M_{B_A^*}\right)^2\right]}, \tag{78}$$

where

$$F_\mathrm{V,A}(0) = \frac{2g_+(0)}{M_B}.$$

We use these in (75) and integrate over x and y in the limit as mentioned in (16) and (17). The IB contribution diverges for the minimum value of x; we take an arbitrary lower limit for x i.e. $x_\mathrm{min} \approx r_l$ for which the divergence problem is cured and the IB part gives some definite value $\mathcal{O}(10^{-20})$. But as the energy of the photon is increased, it approaches zero at x_max. Therefore in the total decay width, this does not contribute much. The SD part is the most dominant part of the decay width which provides almost the whole contribution. This part increases initially with increasing x, reaches its peak value and then starts decreasing. The INT part of the decay width is an increasingly vanishing contribution and can be neglected in comparison to the SD part, because it is suppressed by $\mathcal{O}(10^{-21})$ and becomes flat (approaches zero) as x (the photon energy) approaches 1 (its maxima). Therefore, this does not contribute fairly to the total decay width of the process.

In Fig. 2, the differential decay width of the process is plotted against x, and we see that for our calculations, the peak is shifted to a lower value of x as compared to those for Eilam et al. [11], Korchemsky et al. [13] and Chelkov et al. [14]. So, for the process $B \to \gamma l \nu_l$ the branching ratio obtained is

$$\mathcal{B}(B \to \gamma l \nu_l) = 0.5 \times 10^{-6} \quad (l = \mu). \tag{79}$$

This value is for the form factors given in (77) and (78), which are obtained by restricting to the first radial excitation only. Now if we consider the effect of the second radial excitation the expressions for the form factors are given in (73) and (74). The branching ratios thus obtained are

$$\mathcal{B}(B \to \gamma l \nu_l) = 0.38 \times 10^{-6} \quad (l = \mu,\ A = 3.0),$$
$$\mathcal{B}(B \to \gamma l \nu_l) = 0.32 \times 10^{-6} \quad (l = \mu,\ A = 4.8),$$

for the two representative cases of $A = 3$ and $A = 4.8$ respectively. These are not sensitive to the values of A in contrast to the decay width of $B^* \to B\gamma$. The CLEO Collaboration indicates an upper limit on the branching ratio $\mathcal{B}(B^+ \to \gamma \nu_e e^+)$ of 2.0×10^{-4} at the 90% confidence level [1, 2]. The predicted values are within the upper limit provided by the CLEO Collaboration but differ from those predicted in [13, 14], namely 2–5×10^{-6} and 0.9×10^{-6}, respectively. The Monte Carlo simulation results are given in [39, 40] where the upper limit on the branching ratio for this process is predicted to be 5.2×10^{-5}.

7 Conclusions

Preliminary data from the CLEO Collaboration indicate an upper limit on the branching ratio $\mathcal{B}(B^+ \to \gamma \nu_e e^+)$ of 2.0×10^{-4} at the 90% confidence level [1, 2]. With the better statistics expected from the upcoming

B-factories, the observation and experimental study of this decay could soon become feasible. It is therefore of some interest to have good theoretical control over the theoretical uncertainties affecting the relevant matrix elements.

We have studied the $B \to \gamma l \nu_l$-decay using dispersion relations, asymptotic behavior of the form factors and the Ward identities. The dispersion relation involves the ground state of the B^* and B_A^* resonances and their radial excitations which model contributions from higher states and a continuum contribution, which is calculated from a quark triangle graph. The asymptotic behavior of form factors and Ward identities fixes the normalization of the form factors in terms of the universal function $g_+(0)$ at $q^2 = 0$ and puts constraints on the residues. Thus in our approach, a parameterization of the q^2 dependence of the form factors is not approximated by single pole contributions. This parameterization is dictated by considerations mentioned above and also the coupling constants of the $1^-(B^*)$ and $1^+(B_A^*)$ resonances with the photon are predicted if we restrict ourselves to one radial excitation. By using $\bar{\Lambda} = 0.4\,\mathrm{GeV}^{-1}$ we have calculated $g_+(0) = 0.15$ and predicted the value of $g_{B^*B\gamma} = 5.6\,\mathrm{GeV}^{-1}$ (cf. (67)) and $f_{B_A^*B\gamma} = 6.5 f_B M_{B_A^*}/f_{B_A^*}\,\mathrm{GeV}^{-1}$ (cf. (69)). Taking into account one radial excitation the form factors are summarized in (65) and (66). The branching ratio for the process is then calculated to be $\mathcal{B}(B \to \gamma\nu_l l) = 0.5 \times 10^{-6}$, which lies within the upper limit predicted by the CLEO Collaboration at 90% confidence level [1, 2]. Then we study the effect of a second radial excitation in terms of a single parameter A, which in principle is determined once $g_{B^*B\gamma}$ and $f_{B_A^*B\gamma}$ are known (cf. (71) and (72)). The resulting form factors are given in (73) and (74). By using these form factors the branching ratio is $\mathcal{B}(B \to \gamma\nu_l l) = 0.38 \times 10^{-6}$ and $\mathcal{B}(B \to \gamma\nu_l l) = 0.32 \times 10^{-6}$ for the two representative cases $A = 3.0$ and $A = 4.8$ respectively. These branching ratios are not sensitive to the value of A, in contrast to the radiative coupling constants which give respectively the $B^* \to B\gamma$ width as 23 keV ($A = 0$), 5 keV ($A = 3.0$) and 0.8 keV ($A = 4.8$). One can also predict the radiative widths of the radial excitation in terms of the B^* and B_A^* radiative widths by using (36), (39) and (58). The differential decay width versus photon energy is plotted in Fig. 2 to compare our results with the existing calculations in the light-cone QCD approach [11, 13] and in the instantaneous Bethe–Salpeter approach [14]. The results for $B \to \gamma\nu_l l$ have been reproduced by using Sudakov resummation [13] and have also been shown graphically. In our calculations as well as in [11], the position of the peak of the differential decay width is shifted towards the lower value of the photon energy spectrum. This is due to the double pole in the form factors. The overall effect of the radial excitations is to soften the q^2-behavior of the differential decay distribution, while in [13] it is due to a Sudakov resummation.

Our main inputs have been dispersion relations, asymptotic behavior and Ward identities, all of which have a strong theoretical basis and in these aspects it differs from other approaches. Our approach is closer to the one followed in [19] for $B \to \pi l \nu_l$. The only external parameters involved are f_B, the resonance masses (which are determined in potential models) and $g_{B^*B\gamma}$ and $f_{B_A^*B\gamma}$ which are either predicted or on which we have some theoretical information. The radiative widths of the radial excitations are predicted in terms of the above coupling constants. Thus our approach has predictive power and can be tested by future experiments.

The experiments at the B-factories, BaBar at SLAC and Belle at KEK (Japan) and the planned hadronic accelerators are capable to measure the branching ratio as low as 10^{-8} [41, 42].

Acknowledgements. The work of three of the authors, M.S.K., A.H.S.G. and R., was partially supported by Pakistan Council of Science and Technology and that of M.J.A. by ICSC-World Laboratory fellowship. The authors M.S.K., M.J.A., and A.H.S.G. thank Professor Fayyazuddin for his valuable guidance and helpful discussions. R. and M.J.A. also acknowledge the grant by Higher Education Commission (HEC) under National Distinguished Professorship of R.

References

1. CLEO Collaboration, T.E. Browder et al., Phys. Rev. D **56**, 11 (1997)
2. W.M. Yao et al., J. Phys. G **33**, 1 (2006)
3. G. Burdman, T. Goldman, D. Wyler, Phys. Rev. D **51**, 111 (1995)
4. A. Khodjamirian, G. Stoll, D. Wyler, Phys. Lett. B **358**, 129 (1995) [hep-ph/9506242]
5. E. Lunghi, D. Pirjol, D. Wyler, Nucl. Phys. B **649**, 349 (2003) [hep-ph/0210091]
6. S. Descotes-Genon, C.T. Sachrajda, Nucl. Phys. B **650**, 356 (2003) [hep-ph/0209216]
7. P. Colangelo, F. De Fazio, G. Nardulli, Phys. Lett. B **372**, 331 (1996)
8. P. Colangelo, F. De Fazio, G. Nardulli, Phys. Lett. B **386**, 328 (1996) [hep-ph/9506332]
9. D. Atwood, G. Eilam, A. Soni, Mod. Phys. Lett. A **11**, 1061 (1996)
10. P. Ball, E. Kou, JHEP **0304**, 029 (2003)
11. G. Eilam, I. Halperin, R.R. Mendel, Phys. Lett. B **361**, 137 (1995)
12. C.Q. Geng, C.C. Lih, W.-M. Zhang, Phys. Rev. D **57**, 5697 (1998)
13. G.P. Korchemsky, D. Pirjol, T.-M. Yan, Phys. Rev. D **61**, 114 510 (2000) [hep-ph/9911427]
14. G.A. Chelkov, M.I. Gostkin, Z.K. Silagadze, Phys. Rev. D **64**, 097 503 (2001)
15. N. Cabibbo, Phys. Rev. Lett. **10**, 531 (1963)
16. M. Kobayashi, T. Maskawa, Prog. Theor. Phys. **49**, 652 (1973)
17. T. Goldmann, W.J. Wilson, Phys. Rev. D **15**, 709 (1977) and references therein
18. S. Stone, Heavy Flavor Physics: A Probe of Nature's Grand Design. Varenna, Italy, July 1997 [hep-ph/9709500]
19. G. Burdman, J. Kambor, Phys. Rev. D **55**, 2817 (1997)
20. S.G. Brown, S.A. Bludman, Phys. Rev. B **136**, 1160 (1964)

21. D.A. Bryman, P. Depommier, C. Leroy, Phys. Rep. **88**, 151 (1982)
22. D.Y. Bardin, E.A. Ivanov, Sov. J. Part. Nucl. **7**, 286 (1976)
23. J. Bijnens, G. Ecker, J. Gasser, Nucl. Phys. B **396**, 81 (1993)
24. Riazuddin, Europhys. Lett. **60**, 28 (2002)
25. Riazuddin, T.A. Al-Aithan, A.H.S. Gilani, Int. J. Mod. Phys. A **17**, 4927 (2002) [hep-ph/0007164]
26. N. Paver, Riazuddin, hep-ph/0107330
27. N. Isgur, Phys. Rev. **13**, 129 (1976)
28. N. Isgur, Phys. Rev. D **23**, 817E (1981)
29. G.P. Lepage, S.J. Brodsky, Phys. Lett. B **87**, 359 (1979)
30. G.P. Lepage, S.J. Brodsky, Phys. Rev. D **22**, 2157 (1980)
31. A. Szcizepanick, E.M. Henley, S.J. Brodsky, Phys. Lett. B **243**, 287 (1990)
32. G. Burdman, J.F. Donoghue, Phys. Lett. B **270**, 55 (1970)
33. E. Eichten, C.T. Hill, C. Quigg, The Future of High Energy Sensitive Charm Experiments, ed. by D. Kaplan, S. Kwan (Fermilab Report No. 94/190, Batavia, 1994)
34. A.H.S. Gilani, Riazuddin, T.A. Al-Aithan, JHEP **0309**, 065 (2003) [hep-ph/0304183]
35. E. Eichten, K. Gottfried, T. Kinoshita, K.D. Lane, T.-M. Yan, Phys. Rev. D **21**, 203 (1980)
36. M. Wirbel, B. Stech, M. Bauer, Z. Phys. C **29**, 637 (1985)
37. C.A. Dominguez, N. Paver, DESY Report No: DESY-88-063 (1988)
38. C.A. Dominguez, N. Paver, Z. Phys. C **41**, 217 (1988)
39. M.J. Lattery, Ph.D. thesis (University of Minnesota, 1996)
40. M.A. Shifman, Usp. Fiz. Nauk. **151**, 193 (1987) [Sov. Phys. Usp. **30**, 91 (1987)]
41. G.G. Devidze, ICTP preprint: IC/2000/71 (2000)
42. G.G. Devidze, hep-ph/9905431